Riluzole, a glutamate modulator, slows cerebral glucose metabolism decline in patients with Alzheimer's disease

Dawn C. Matthews,[1] Xiangling Mao,[2] Kathleen Dowd,[3] Diamanto Tsakanikas,[3] Caroline S. Jiang,[3] Caroline Meuser,[4] Randolph D. Andrews,[1] Ana S. Lukic,[1] Jihyun Lee,[2] Nicholas Hampilos,[2] Neeva Shafiian,[5,6] Mary Sano,[4] P. David Mozley,[2] Howard Fillit,[7] Bruce S. McEwen,[3,†] Dikoma C. Shungu[2] and Ana C. Pereira[3,5,6,8]

[†]**Deceased.**

Abstract

Dysregulation of glutamatergic neural circuits has been implicated in a cycle of toxicity, believed among the neurobiological underpinning of Alzheimer's disease. Previously, we reported preclinical evidence that the glutamate modulator riluzole, which is FDA-approved for the treatment of amyotrophic lateral sclerosis, has potential benefits on cognition, structural and molecular markers of aging and Alzheimer's disease. The objective of this study was to evaluate in a pilot clinical trial, using neuroimaging biomarkers, the potential efficacy and safety of riluzole in patients with Alzheimer's disease as compared to placebo. A 6-month phase 2 double-blind, randomized, placebo-controlled study was conducted at two sites. Participants consisted of males and females, 50 to 95 years of age, with a clinical diagnosis of probable Alzheimer's disease, and Mini-Mental State Examination between 19 and 27. Ninety-four participants were screened, fifty subjects that met inclusion criteria were randomly assigned to receive 50mg riluzole (n=26) or placebo (n=24) twice a day. Twenty-two riluzole-treated and 20 placebo participants completed the study. Primary endpoints were baseline to 6 months changes in a) cerebral glucose metabolism as measured with fluorodeoxyglucose-positron emission tomography in pre-specified regions of interest (hippocampus, posterior cingulate, precuneus, lateral temporal, inferior parietal, frontal) and b) changes in posterior cingulate levels of the neuronal viability marker N-acetylaspartate as measured with in vivo proton magnetic resonance spectroscopy. Secondary outcome measures were neuropsychological testing for correlation with neuroimaging biomarkers and in vivo measures of glutamate in posterior

cingulate measured with magnetic resonance spectroscopy as a potential marker of target engagement. Measures of cerebral glucose metabolism, a well-established Alzheimer's disease biomarker and predictor of disease progression, declined significantly less in several pre-specified regions of interest with the most robust effect in posterior cingulate, and effects in precuneus, lateral temporal, right hippocampus and frontal cortex in riluzole-treated subjects in comparison to placebo group. No group effect was found in measures of N-acetylaspartate levels. A positive correlation was observed between cognitive measures and regional cerebral glucose metabolism. A group by visit interaction was observed in glutamate levels in posterior cingulate, potentially suggesting engagement of glutamatergic system by riluzole. In vivo glutamate levels positively correlated with cognitive performance. These findings support our main primary hypothesis that cerebral glucose metabolism would be better preserved in the riluzole treated group than in the placebo group and investigations in future larger and longer studies to test riluzole as a potential novel therapeutic intervention for Alzheimer's disease.

Author affiliations:

1 ADM Diagnostics Inc., Northbrook, IL, 60062 USA

2 Department of Radiology, Weill Cornell Medicine, New York, NY, 10021 USA

3 The Rockefeller University, New York, NY, 10065 USA

4 Department of Psychiatry, Alzheimer's Disease Research Center, Icahn School of Medicine at Mount Sinai, New York, NY, 10029 USA

5 Department of Neurology, Friedman Brain Institute, Icahn School of Medicine at Mount Sinai, New York, NY, 10029 USA

6 Nash Family Department of Neuroscience, Friedman Brain Institute, Icahn School of Medicine at Mount Sinai, New York, NY, 10029 USA

7 Alzheimer's Drug Discovery Foundation, New York, NY, 10019 USA

8 Ronald M. Loeb Center for Alzheimer's Disease, Icahn School of Medicine at Mount Sinai, New York, NY, 10029, USA

Correspondence to: Dr. Ana. C. Pereira

Department of Neurology, Icahn School of Medicine at Mount Sinai, 1468 Madison Avenue, New York, NY, 10029, USA
E-mail: ana.pereira@mssm.edu

Keywords: Alzheimer's disease; riluzole; cerebral brain metabolism; FDG-PET; glutamate

Introduction

Alzheimer's disease (AD) is the most common neurodegenerative disorder, affecting over 43 million people worldwide with enormous psychosocial and economic impact upon society [1]. Without effective therapies and given a high rate of clinical trial failures, an urgent need remains to identify treatment strategies that can slow progression of AD neurodegeneration. In this exploratory clinical trial, we evaluated the potential of riluzole, a glutamate modulator that exhibits neuroprotective properties and is approved for amyotrophic lateral sclerosis (ALS), to provide benefit in AD.

Glutamatergic pyramidal neurons that furnish corticocortical connections between association cortical areas and the excitatory hippocampal connections that subserve memory and cognition are the most vulnerable to damage and loss in AD [2, 3]. The entorhinal cortex, an early site of tau accumulation, consists primarily of pyramidal cells that utilize glutamate as an excitatory neurotransmitter [4]. The hippocampal and neocortical atrophy characteristic of AD progression demonstrate degeneration predominantly in large glutamatergic pyramidal neurons [5-7]. Glutamate-mediated toxicity has been implicated as one potential mechanism of neuronal loss in AD [8]. Glutamate overflow to extrasynaptic space and activation of extrasynaptic NMDA receptors has been hypothesized to allow excessive sodium and calcium influx, degrading mitochondrial function and leading to apoptosis [9]. We have previously shown that downregulation of the major glutamate transporter EAAT2 (or GLT-1) accelerates age-related cognitive decline, and conditional heterozygous astrocytic EAAT2 knockout mice have dysregulated immune signaling that correlated with cognitive performance [10]. The neuropathophysiological hallmarks of AD,

amyloid-β (Aβ) plaques and neurofibrillary tangles (NFT) formed of hyperphosphorylated tau, have been implicated in glutamatergic dysfunction. NFT tend to preferentially accumulate in excitatory pyramidal neurons [11] [12, 13]. Tau gene expression and phosphorylation are increased in the setting of glutamate toxicity [14, 15] and tau release and propagation through interconnected neural circuits are dependent on neuronal activity [16-18]. Oligomers of Aβ disrupt glutamate transporters [19], leading to spillover and activation of extrasynaptic NMDA receptors, implicated in glutamate-mediated toxicity and inhibition of long term potentiation (LTP) [20]. Aβ release is dependent on neuronal activity [21] and decreases surface expression of synaptic NMDA receptors [22], critical for physiologic neurotransmission. Glutamatergic dysregulation thus forms a cycle of toxicity in AD. We have hypothesized that pharmacologic modulation of glutamatergic neural circuits in AD could diminish toxicity through one or more of these pathways, with the potential to preserve or increase neuronal function. Particularly relevant would be protection of the pyramidal neurons that are most vulnerable in AD, through reduced glutamate overflow to extrasynaptic space, reducing glutamate-mediated toxicity and potentially allowing increased synaptic activity.

Our group has previously shown that riluzole can prevent age-related cognitive decline in rodents through clustering of dendritic spines [23], strengthening neural communication [24, 25]. Furthermore, we have shown that riluzole rescues gene expression profiles related to aging and AD, and that the most affected pathways were related to neurotransmission and neuroplasticity [26]. More recently, we have demonstrated that riluzole prevented hippocampal-dependent spatial memory decline in an early-onset aggressive mouse model of AD (5XFAD), reduced amyloid pathology, and reversed many of the gene expression changes in immune pathways [27]. These reversals involved microglia-related genes [27] thought to be critical mediators of AD pathophysiology [28-30], including a recently identified unique population of disease-associated microglia (DAM) [31]. Riluzole has also been reported to reduce total tau [32], which in clinical studies correlates with glucose metabolism and cognition [33]. Riluzole has been demonstrated to modulate ion channels [34, 35], and to increase neurotrophic factors [36, 37].

Prior research suggests that riluzole-related improvements in astrocytic function and glutamate uptake may produce changes detectable with FDG PET measurement of glucose metabolism and with magnetic resonance spectroscopy (^{1}H MRS) [38]. This may occur through increased activity of the main glutamate transporter in the brain, EAAT2 and glutamate uptake [32, 39-41]. In rodent models, riluzole increases glutamate uptake by astrocytes and mitigates astrocytic dysfunction [39]. A tight coupling between glutamatergic activity and cerebral glucose metabolism with stoichiometry close to 1:1 has been demonstrated [42]. Glutamatergic transmission accounts for more than 80% of ATP generated from brain metabolism [43]. In one pathway, astrocytic uptake of glutamate released by neuronal synaptic activity leads to conversion of glucose to lactate by the astrocyte, which is transported to neurons and converted to pyruvate for ATP production [44]. Direct metabolism of glucose by neurons has been described and likewise supports the 1:1 relationship between increases in the glutamate−glutamine cycle and neuronal glucose oxidation [45]. In a ^{1}H-[^{13}C] MRS study conducted in rats, riluzole administration increased glutamate-C4, GABA-C2, and glutamine-C4 in hippocampus and prefrontal cortex, demonstrating increased glucose oxidative metabolism and glutamate/glutamine cycling between neurons and astroglia [38].

In the current study, we aimed to translate preclinical findings to human AD through a pilot phase 2 randomised, double-blind, placebo-controlled clinical trial of riluzole in patients with a diagnosis of mild Alzheimer's disease. We tested the hypotheses that (a) riluzole would mitigate the decline of regional cerebral glucose metabolism in AD as measured with FDG PET, a well-established biomarker in AD, (b) FDG PET metabolic brain maps would correlate with cognitive measures and, (c) riluzole would alter the neuronal viability marker, N-acetylaspartate (NAA), and glutamate levels as a marker of target engagement, both measured with ^{1}H MRS.

Materials and methods

Study design and participants

Patients with a clinical diagnosis of probable Alzheimer's disease based upon neurological and neuropsychological evaluation (National Institute on Aging - Alzheimer's disease Association, NINCDS-ADRDA criteria) [46, 47], Mini Mental State Examination (MMSE) score of 19 to 27, and 50 to 95 years were enrolled in this pilot phase 2 double-blind, randomized, placebo-controlled study. For inclusion, FDG PET baseline scans were also evaluated to confirm a lack of a frontotemporal dementia or Lewy body disease pattern of hypometabolism. All subjects were stable on acetylcholinesterase (AChE) inhibitors for at least 2 months before starting the trial and continued to take AChE throughout the study with the exception of one subject who had never been on AChE therapy. The study was conducted at two sites (Rockefeller University Hospital and Icahn School of Medicine at Mount Sinai, both in New York City), with the approval of the Institutional Review Boards (IRB) of both Institutions. All neuroimaging was performed at Citigroup Biomedical Imaging at Weill Cornell Medicine under an IRB protocol separetely approved by that Institution. Memantine, which acts on the glutamatergic system through a different mechanism than riluzole, was not allowed for 6-weeks prior to study entrance nor during the study duration. Other exclusion criteria were: abnormal liver function (>2 times the upper limit of normal for alanine aminotransferase (ALT) or aspartate aminotransferase (AST); or bilirubin >1.5 times the upper limit of normal, positive Hepatitis Serology (Hep. B antigen+ or Hep. C antibody+), uncontrolled diabetes mellitus (Hba1c>7), chronically uncontrolled hypertension, MRI contraindication, history of brain disease, current smoker or user of nicotine-containing products, currently taking medications with evidence of glutamatergic activity or effects on brain glutamate levels such as lamotrigine, lithium, opiates, psychostimulants such as amphetamines and methylphenidate, tricyclic antidepressants, benzodiazepines and any other drug that the investigators judged might interfere with the study (subjects on those medications could be included in the study but without MRS measurements) and others (full criteria at clinicaltrial.gov NCT01703117).

Participants were randomly assigned in a double-blind fashion to receive riluzole at a dose of 50mg twice a day or placebo for 6 months, with age-matched cohorts of 50-74 and 75-95 years old. Written informed consent was obtained from participants or their legally authorized representative before initiation of study procedures. Data were periodically

reviewed by the study Data Safety and Monitoring Board (DSMB). Two participants had a delay in endpoint due to COVID-19 pandemic (see statistical analysis).

Randomization and Blinding

Random codes were generated by the hospital pharmacy prior to study initiation, using fixed seed numbers and validated randomization software, and used in sequence. In each of the two age groups, 24 subject numbers were randomized into balanced blocks of either 2 or 4, which were randomly assigned. Study capsule dosage forms (active and placebo) were prepared by pharmacy staff in a blinded manner using over-encapsulation, and opaque (size 3 capsule shells with Lactose NF as an excipient at Rockefeller University Hospital and 0 capsule shells with microcrystalline cellulose as an excipient at Mount Sinai Hospital). The active drug product contained FDA approved riluzole 50 mg tablets. For ease of use and compliance, the pharmacy packaged the blinded capsules into medication bottles or organizer trays. Bottles or trays were labeled in a blinded manner, and included patient name, visit, and per protocol dosing instructions. Returned trays/bottles were collected by the pharmacy and patient returns, including capsule counts, were recorded by the pharmacy. All encapsulation, packaging, and labeling procedures were double verified by pharmacy staff prior to dispensing.

Procedures

All study personnel had training on study procedures and assessments. A board-certified neurologist made a neurological assessment and administered the MMSE to all subjects. FDG PET scans were acquired at baseline and at six months. ^{1}H MRS was performed at baseline, three months, and six months. A neuropsychological testing battery was performed by a licensed neuropsychologist at Rockefeller University and supervised by one at Mount Sinai at baseline, three months, and six months. Patients were seen once a month in clinic for clinical assessment and blood samples were obtained at every visit for safety laboratory exams; blood test results were evaluated by a physician not directly involved in the study in order to maintain physician-investigators blind.

Outcome Measures

Primary endpoints were (1) change from baseline to 6 months in cerebral glucose metabolism measured with FDG PET in posterior cingulate cortex, hippocampus, precuneus, and medial temporal, lateral temporal, inferior parietal, and frontal lobes, referred to collectively as our pre-specified regions of interest; and (2) changes in ^{1}H MRS measures of NAA in posterior cingulate at six months. Secondary outcome measures were neuropsychological testing (Alzheimer's Disease Assessment Scale- Cognitive Subscale – ADAScog [48, 49], ADCS Activities of Daily Living – ADL Inventory [50], Neuropsychiatry Inventory – NPI) [51] total and other measures of memory, executive, visuospatial, attention and language functions for correlation with neuroimaging biomarkers. Another secondary outcome measure was in vivo measurement of glutamate with ^{1}H MRS in posterior cingulate as a marker of target engagement at three and six months compared to baseline. ^{1}H MRS measures were obtained in bilateral hippocampi as a pre-defined exploratory outcome. Each FDG PET image was also analyzed using a previously developed AD Progression Classifier **(Figure 1A[ii])** that quantifies the degree to which a pattern of hypometabolism and preservation relative to whole brain is expressed [52]. Increases in classifier score correspond to increased expression of a pattern of hypometabolism that corresponds to the progression of AD as validated using over 500 ADNI subjects [52].

As post-hoc exploratory analyses, relationships between the FDG PET and MRS measures and the cognitive endpoints were examined. NPI scores and FDG PET in the orbitofrontal cortex, a region associated with disinhibition, apathy, and other neuropsychiatric attributes [53, 54], were examined for potential association. MRS outcomes in NAA were evaluated at three months, and total creatinine (tCr), and other brain metabolites were examined at three and six months. A composite subregion of posterior cingulate and inferior precuneus was measured on post-hoc basis to maximize spatial overlap with the boundaries defined in the MRS scans. Subgroup analyses were conducted, stratified by ApoE4 carrier status, age group, and sex. Age was of interest due to differences in clinical rates of decline and in the distribution of tau pathology in younger vs. older AD patients [55].

FDG PET Methods

For each FDG PET scan, 5 mCi of florodeoxyglucose was administered followed by a 40 minute uptake period during which the participant was in a resting state with eyes and ears open, without activity or audiovisual distraction. Images were acquired on a Siemens Biograph 64mCT scanner as a series of 4 frames of 5 minutes each. In some initial cases, a full dynamic scan was performed and late timeframes were extracted for processing and analysis.

All PET images were inspected for motion or artifact. Using SPM12 (Wellcome Trust), motion correction was performed and frames averaged into a static image. Each 6 month scan was coregistered to the baseline FDG scan, which was co-registered to the participant's T1-weighted MRI scan. MRI scans were segmented into gray, white, and CSF tissue and spatially transformed to a template in MNI space, and the spatial transformations applied to the PET scans. Regions of interest **(Figure 1A[i])** adapted from Freesurfer [56, 57] atlases were thresholded with a smoothed gray participant-specific segment and average intensities within each region of interest were measured. A reference region for calculation of Standardized Uptake Value Ratios (SUVRs) was defined based upon preserved voxels in the AD Progression Classifier, most pronounced in the paracentral region. Longitudinal changes in SUVRs using this reference were compared to SUVRs referenced to (separately) centrum semiovale white matter, cerebellum, pons, and whole brain. While these regions tend to be more variable due to technical factors (cerebellum, pons), progressive hypometabolism effects (whole brain), or potentially affected by riluzole (cerebellum) [58], consistency in results could help to confirm the robustness of findings. Images were also evaluated (scored) using the FDG AD Progression classifier.

MRI and ^{1}H MRS methods

All MRS neuroimaging studies were conducted on a multinuclear 3.0T GE SIGNA HDx or Discovery MR750 system. Each enrolled subject underwent high resolution axial T_1-, T_2- and spin density-weighted scans. These images were used to prescribe the voxels of interest for the ^{1}H MRS scans. A T_1-weighted volumetric scan was acquired using a spoiled gradient-recalled echo sequence (SPGR, TR 12.21 ms, TE 5.18 ms, flip angle = 7, voxels

0.94 x 0.94 x 1.5mm) on the GE HDx system or a magnetization-prepared rapid gradient-echo sequence (MPRAGE, TR 8.34 ms, TE 1.7 ms, flip angle = 7, voxels 0.94 x 0.94 x 1.5mm) on the GE Discovery MR750, along with an axial fast Fluid-Attenuated Inversion Recovery (FLAIR) scan for brain tissue segmentation and use in PET image co-registration and region of interest definition, and to rule out exclusionary focal brain lesions.

In vivo brain levels of glutamate, NAA, tCr and other major metabolites were obtained using ^{1}H MRS and a 2x2x2-cm^{3} Posterior Cingulate Cortex (PC) voxel of interest (**Figure 1B[i-iii]**, in approximately 6.5 minutes using the constant-time point-resolved spectroscopy (CT-PRESS) technique [59, 60] with TE 30 ms, 129 constant-time increments (t1) of 0.8ms, and TR 1500 ms and a receive-only 8-channel phased-array head coil, as we recently described [61]. The distinguishing feature of CT-PRESS is that it enables MRS measurement of glutamate uncontaminated by glutamine [59, 60]. **Figure 1B[iv]**, presents a sample posterior cingulate cortex CT-PRESS spectrum acquired in 6 min, and its processing to derive the levels of the metabolites of interest.
Methods for ^{1}H MRS of Hippocampi obtained for exploratory analysis are in the Supplementary Information.

^{1}H MRS Data Processing and Quantification

Using previously described spectral quality assessment criteria [62], the areas of the individual spectral peaks, which are proportional to their respective concentrations, were obtained by frequency-domain fitting each resonance to a Gauss-Lorentz (i.e., pseudo-Voigt) lineshape function using the Levenberg-Marquardt nonlinear least-squares algorithm as implemented in ^{1}H MRS data processing software written in IDL [62] and illustrated in **Figure 1B[iv] and Supplementary Figure 2 A[d]** for CT-PRESS and J-edited spectra, respectively. The levels of NAA, glutamate, GABA, Glx and other metabolites were expressed semi-quantitatively as ratios of peak areas relative to that of the unsuppressed water signal (W) from the same voxels, as previously described [62]. For consistency with earlier MRS literature, levels of the same metabolites were also expressed as peak ratios relative to tCr area in the same voxel. To estimate the proportions of gray matter (GM), white matter (WM) and cerebrospinal fluid (CSF) contained in the voxels of

interest, SPM8 (http://www.fil.ion.ucl.ac.uk/spm) and in-house program in MATLAB (https://www.mathworks.com/products/matlab.html) were used to generate the proportions of GM, WM, and CSF for each voxel.

Data availability

Anonymized data will be shared by request from a qualified academic investigator for the sole purpose of replicating procedures and results presented in the article and as long as data transfer is in agreement with IRB of the involved Institutions, which should be regulated in a material transfer agreement.

Statistical Analysis

Placebo and treatment groups were compared to identify potential baseline differences in region of interest SUVRs and in age, sex, ApoE4 dose and carrier status, and MMSE score. The 6-month change in SUVR in each region of interest was compared across groups using a one-way ANCOVA model with the change in SUVR value as the dependent variable, study arm as the categorical independent variable, and baseline SUVR value as a continuous variable covariate (JMP v15, SAS software) (Results were consistent with use of post-treatment SUVR as the independent variable). Age, gender, ApoE4 carrier status, and baseline MMSE were investigated as covariates. Assumptions including normal distribution, homogeneity of variance, and linear correlation between baseline and post-treatment SUVR were verified, and the number of covariates in a given parametric model was limited to 1-3. Non-parametric tests were applied depending upon the number of subjects per analysis group and other assumption tests. Effect sizes were calculated using Cohen's d (d). For the two participants who received their FDG PET scan 2 and 3 months after the 6-month timepoint due to restrictions arising from COVID 19, the change in value was adjusted using a linear proportional reduction (e.g. value x 6/8 or 6/9). Groups were evaluated post-hoc without these two participants. ^{1}H MRS data, with three timepoints, were analyzed using linear mixed effects models with group, timepoint, and group-by-timepoint interaction as fixed effects and subject as a random effect (SAS Studio v3.8). In this exploratory study, a P-value of less than 0.05 was considered significant and correction

for multiple comparisons was not pre-specified. However, results using a Bonferroni correction for multiple comparisons were also reported for significant primary endpoints.

Non-prespecified FDG and MRS data were evaluated in the same manner as pre-specified outcomes, without correction for multiple comparisons. The study was not statistically powered for clinical endpoints or these additional MRS measures, but directional trends were examined for potential effect.

Results

Sample Characteristics and Demographics

A total of 94 participants were screened at the two performance sites, of which 44 did not meet inclusion/exclusion criteria. The remaining 50 participants were randomly assigned to receive riluzole (n=26) or placebo (n=24). Of these, 22 patients receiving riluzole and 20 patients receiving placebo completed the study and had both FDG PET timepoints. The diagram of **Figure 2** shows the subject disposition.

Enrolled subjects were 26 female and 16 male, age 58 to 88, and 58% apolipoprotein 4 (ApoE4) carriers (Table 1, 1 subject unavailable). There were no significant between–group differences in baseline characteristics of the patients with respect to age, sex, education or ApoE4, although there was a trend for a greater proportion of ApoE4 carriers in the riluzole group. Baseline neuropsychological measures were well balanced for MMSE, NPI, ADL total, CDR total in riluzole group in comparison to placebo; however, the riluzole group trended as more impaired in ADAS-cog than placebo at baseline (p=0.08); Table 1).

Neuroimaging Outcome Measures

FDG PET

The study's main primary outcome measure confirmed a difference between arms in FDG PET cerebral metabolic changes over the 6 month treatment period, with less decline in multiple pre-specified brain regions in the riluzole group in comparison to placebo group. There were no significant or trend level differences between study arms at baseline in the regional SUVRs that were compared, or in the FDG AD Progression score. Given the trend level difference between study arms in ApoE4 dose, analyses were performed and compared with and without its inclusion as a covariate. **Supplementary Table 3** presents the mean, standard deviation, and significance findings for the FDG PET comparisons. Posterior cingulate (PC) glucose metabolism, a primary endpoint, was significantly preserved in riluzole-treated group in comparison to placebo over the 6 month period (effect size (d) 1.31; P<0.0002 with ApoE4 dose included as covariate, P<0.0003 without ApoE4 dose included, with the effect significant using any of several different reference regions (paracentral p<0.0002, centrum ovale p<0.008, whole brain p<0.016, cerebellar cortex p<0.03)**; Figure 3A-C**. PC significance readily survived Bonferroni correction for multiple comparisons. Regional cerebral glucose metabolism was more preserved in the riluzole group in comparison to placebo in several other pre-specified regions of interest including precuneus (P<0.007, d=0.84), lateral temporal (P<0.014, d=0.80), right hippocampus (P<0.025, d=0.72), and frontal cortex (P<0.035, d=0.67), and the exploratory subregions of orbitofrontal cortex (P<0.008, d=0.86**)** and posterior cingulate-precuneus subregion (P<0.007, d=0.88)**; Figure 4**. A majority of these still showed trend level significance if corrected for multiple comparisons. Age, sex, education, and ApoE4 dose were not significant contributors to treatment effect. No differences were observed in control regions such as subcortical white matter, pons, and cerebellar vermis.

When groups were stratified and analyzed separately on a post-hoc basis (using nonparametric tests due to subgroup size) by ApoE4 carrier status, age, and sex, the treatment effect of riluzole group having less decline than placebo was observed in both ApoE4 carriers and non-carriers (P<0.004 in carriers (N=8 placebo, 15 riluzole, effect size 1.526) and P<0.09 in non-carriers (N=11 placebo, 7 riluzole, d=0.89), in both younger and older groups (P<0.002 in older group, N=13 placebo, 15 riluzole, d=1.370 and P<0.08 in younger group, N=7 placebo and 7 riluzole, d=0.96) **(Figure 3D)**, and in males and females

(both groups p<0.02; N=14 placebo, 12 riluzole in female group and N=6 placebo, 10 riluzole in the male group). Inclusion of ApoE4 dose in the by-age group analysis increased the p value for study arm to 0.13 in the younger group, with ApoE4 dose showing a trend level influence in this age group (P<0.07) but not the older age group (P<0.78). Inclusion of ApoE4 dose in the by-sex group analysis decreased the P value for study arm to P<0.008 in the female group, with ApoE4 dose showing a trend level influence in the female group (P<0.09) but not the male group (P<0.84).

FDG PET measures have been shown to correlate with cognitive decline and predict disease progression [63-65]. The exploratory FDG PET progression classifier score analyses showed a trend of less increase (less worsening) in AD progression score in the riluzole group in comparison to placebo (P<0.07, **Figure 5A**). There was a trend level greater difference between arms in ApoE4 carriers than noncarriers. FDG PET AD progression scores correlated with ADAS-cog at baseline (all subjects R=0.61, P<0.00002; placebo group R=0.57, P<0.008; riluzole group R=0.48, P<0.0004) and changes in FDG AD progression scores correlated with changes in ADAScog (all subjects R=0.46, p<0.002; placebo group R=0.56, P<0.011; riluzole group R=0.29, not significant, and reduced range of score increases) **(Figure 5B**) over the 6 months of the study. Additional correlations were observed between FDG PET and cognitive measures as shown in **Figure 6**, including relationships between baseline FDG AD Progression score and MMSE (R=0.61, P<0.00002, **Figure 6A**), FDG PC SUVR and MMSE (R=0.35, P<0.00003, **Figure 6B**), lateral temporal SUVR and ADAS-cog (R=0.54, P<0.0002, **Figure 6C**) and orbitofrontal SUVR and NPI score (R=0.52, P<0.0004, **Figure 6D**). The robust correlations observed between FDG PET brain metabolism and cognitive measures in our dataset support our secondary outcome measure related to neuropsychological assessment.

^{1}H MRS

Voxel Tissue Composition and spectral quality

The proportions of gray matter, white matter or cerebrospinal fluid in the posterior cingulate or the hippocampal voxels did not differ between groups. Except for an inconsequential increase in the full width at half maximum (FWHM) of the posterior

cingulate water resonance between baseline (4.5Hz) and 6 months (6Hz), the spectral quality parameters were remarkably stable, with no group differences in the unsuppressed reference tissue water signal (W) or signal-to-noise ratios observed as a function of time in any of the voxels. The voxel tissue composition and spectral quality control data are summarized in **Supplementary Table 2**.

Posterior Cingulate ^{1}H MRS Results

As a primary endpoint, neither NAA/W nor NAA/tCr showed a temporal change (group by visit interaction: P=0.14 or P=0.89, respectively) **(Supplementary Figure 1**). ^{1}H MRS results in secondary endpoint posterior cingulate Glutamate (Glu) levels showed a group by visit interaction when expressed as Glu/tCr (P=0.05) and a trend-level interaction when expressed as Glu/W (P=0.3), with both levels increasing after the first 3 months of treatment (**Figure 7A**). No significant changes from baseline to 6 months were observed. In post-hoc analyses, within the riluzole group NAA/W and Glu/W levels were correlated positively for all three time points, while NAA/tCr and Glu/tCr were positively correlated at baseline (**Figure 7B**). Within the placebo group, both NAA/W vs. Glu/W and NAA/tCr vs. Glu/tCr were positively correlated for all three time points **(Figure 7B**).^{1}H MRS measures of Glu/W correlated positively with MMSE and negatively with ADAS-cog across all subjects (**Figure 7C)**. Across all subjects Glu/tCr positively correlated with MMSE (P=0.01) but not ADAS-cog (P=0.39).

Hippocampal ^{1}H MRS Results

On an exploratory basis, a significant increase in GABA/W was observed in the left hippocampus with a significant group by visit interaction (P=0.03) (**Supplementary Figure 2B**) as a trend in GABA/tCr (P=0.3). Left hippocampus GABA/W levels positively correlated with memory performance; see Logical Memory 1 and 2 testing correlations at baseline in **Supplementary Figure 2C**. No significant changes were seen in any measure of Glx or NAA levels in right or left hippocampus nor GABA levels in right hippocampus.

Neuropsychological testing was a secondary measure for correlation with neuroimaging biomarkers although the study was not powered for a significant neuropsychological effect.

Trend level findings are shown in **Supplementary Figure 3** for the key functional measures of ADL Inventory, NPI and ADAS-cog.

Adverse Events

There were no statistical differences in adverse events between treatment groups, with 23 of 26 patients (88.5%) in the riluzole group and 22 of 24 (91.7%) in the placebo group having at least one adverse event during the study. Serious adverse events occurred in 2 (7.7%) in the riluzole group and 1 (4.2%) in the placebo group.The most common side effects in the riluzole group consisted of abdominal discomfort (15.4% in riluzole, none in placebo); diarrhea (15.4% in riluzole, 8.3% in placebo); dizziness (15.4% in riluzole, 4.2% in placebo); urinary frequency (11.5% in riluzole and none in placebo), nausea (7.7% in riluzole, none in placebo), cough (19.23% in riluzole, 12.5% in placebo), elevated liver enzymes (7.7% in riluzole and 4.2% in placebo) and others **(Supplementary Table 1)**. Among the randomized patients, 4 of 26 (15.4%) in the riluzole group and 3 of 24 (12.5%) in the placebo group had an adverse event that led to removal from the trial. There were no significant differences in the frequency of participants who were discontinued from the trial due to adverse events.

Discussion

The results of this pilot double-blind, randomized, placebo-controlled trial of riluzole 50mg twice daily in Alzheimer's disease patients have confirmed our primary hypotheses, showing 6 months of riluzole treatment to be associated with less decline in FDG PET measures of cerebral glucose metabolism compared to placebo. The effect was most robust in posterior cingulate, but effects were also observed in precuneus, lateral temporal cortex, right hippocampus and frontal cortex. Glutamate levels measures with ^{1}H MRS, a secondary outcome, showed a significant or trend-level group by visit interaction in posterior cingulate, whereby the levels of this excitatory animo acid neurotransmitter increased after three months of treatment, suggesting the possibility that riluzole engages

the glutamatergic system as its therapeutic target. No changes were found in the ^{1}H MRS levels of NAA, our second primary outcome measure. A significant correlation was observed between cognitive measures and cerebral metabolism in FDG PET, a key measure of brain function in AD. Posterior cingulate glutamate levels also correlated with cognitive performance. Our study provides the first in-human data supporting a potential therapeutic benefit of riluzole in patients with Alzheimer's disease.

The beneficial effects of riluzole upon neuronal function and cognition observed in this pilot study could be attributable to one or more of the mechanisms that have been established in rodent models. In this mild AD population, where amyloid and tau were already well-established, the most likely mechanisms of therapeutic effect by riluzole could have been in preventing further damage to vulnerable pyramidal neurons through modulation of glutamate levels, reduced glutamate-mediated toxicity, and increased synaptic activity. The directional favorable cognitive effects are consistent with the prevention of age-related cognitive decline found in rodent models [27, 66].

Similar effects upon glucose metabolism were observed with riluzole as those reported for memantine in AD patients over the same time period [67], with both studies finding greatest effects in posterior cingulate and precuneus. Memantine acts on the glutamatergic system through NMDA receptor partial antagonism, reducing calcium ion influx and related toxicity [68]. Riluzole has shown similar mitigating effects upon sodium and calcium ion influx, through protein kinase C (PKC) inhibition or by regulating glutamate transporter and modulation of ion channels leading to potential decreased glutamate overflow to extrasynaptic space rather than direct NMDA interaction [69]. Given memantine's effects upon glucose metabolism, this mitigation may also have contributed to the effects of riluzole. The numerous effects of riluzole demonstrated preclinically may support additional therapeutic benefit in AD.

FDG PET was chosen as the main primary outcome measure in this study because it is a well-established biomarker of neuronal function in AD [65, 70], and progressive

hypometabolism in AD-relevant regions strongly correlates with clinical progression [63-65]. The posterior cingulate, in which the most robust treatment effect was observed in this study (**Figure 3 A-C**), is a hub network region and one of the earliest and most strongly affected regions in AD [71, 72]. The slower decline in cerebral glucose metabolism with riluzole was observed in both younger and older groups, males and females, and APOE4 carriers and non-carriers (**Figure 3D**).

The observed lessening of metabolic decline in the riluzole group compared to placebo in several AD-related regions of interest **(Figure 4)** suggested an effect in AD-related networks. Consistent with this, the AD progression classifier score, previously validated in ADNI subjects [52], showed a trend-level slower disease progression in the riluzole-treated group than in the placebo group **(Figure 5A**). This preservation supports further exploration of the apparent disease-modifying effect of riluzole in larger, longer, full-efficacy clinical trials, with assessments of clinical and neuroimaging changes at multiple time points to map the trajectory of therapeutic response. The less robust though significant effects in the AD-related regions other than PC and precuneus may reflect technical factors including greater variability due to rotational head motion and differences in slice location from the reference region.

The trend-level differences in longitudinal AD progression pattern expression between ApoE4 carriers and non-carriers merits further study. A potential explanation may be due to baseline neural hyperexcitability in ApoE4 carriers [73, 74] that could be more responsive to glutamatergic modulation. It would be of interest to characterize AD patients for analysis stratification, as the population is highly heterogeneous with regard to clinical manifestations, rate of disease progression, tau burden, comorbidities, and possibly treatment response. This heterogeneity was present in our study.

We observed a strong correlation between the FDG PET AD Progression Classifier score and ADAS-cog at baseline and in treatment change from baseline to 6 months **(Figure 5B).** This is consistent with previous findings in the ADNI and other populations [52], and suggests that FDG PET progression scores are predictive of and aligned with cognitive changes.

Examining placebo and riluzole groups separately, correlations at baseline were significant for both groups. Additional associations between FDG-PET glucose metabolism and cognitive measures at baseline were observed **(Figure 6**). Use of biomarkers to predict cognitive effects in smaller trials could potentially lower clinical trial costs and play an important role in identifying which therapies should be advanced to larger trials.

^{1}H MRS has shown metabolic differences in AD compared to matched normal individuals [75], however, the results have not been sufficiently consistent to enable their use as reliable outcome measures in AD in a manner analogous to FDG PET measures of cerebral glucose metabolism. For example, in a study of memantine that showed no MRS effects despite favorable glucose metabolism effects, the authors noted that MRS results were affected by variability and patient-induced artifacts [76]. With riluzole an established glutamate modulator, this study sought to derive objective evidence of riluzole treatment target engagement by using ^{1}H MRS as a secondary outcome measure to measure in vivo brain levels of glutamatergic compounds. Our finding of a significant or trend-level group by visit interaction for posterior cingulate glutamate, with its levels rising between month 3 and 6 months of treatment **(Figure 7A**) suggest potential engagement of the glutamatergic system by riluzole. This interpretion should be made with caution as it is a significance in a group by visit interaction and preliminary while there were no significant differences between groups from baseline to 6 months as originally hypothesized. It has been hypothesized that enhancing the efficiency of glutamatergic synaptic activity, which riluzole is postulated to accomplish, leads to an increase in intracellular glutamate levels [77], which was likely the major contributor to the detected ^{1}H MRS glutamate signal. We sought to assess the effects of riluzole on neuronal viability and function through simultaneous ^{1}H MRS measurement of the putative neuronal marker NAA, but did not detect changes in NAA. Negative findings have also been reported in prior longitudinal ^{1}H MRS studies of AD and ALS, which revealed cross-sectional but not longitudinal NAA changes, and attributed this to inter-subject variability and technical factors [78, 79]. Depleted ^{1}H MRS levels of NAA and glutamate have been reported in AD compared to healthy controls [75, 80, 81], which could not be assessed in this study due to the lack of a normal comparison group. We observed an exploratory correlation between glutamate levels and

cognitive measures in posterior cingulate such as MMSE and ADAS-cog (**Figure 7C**), with higher ^{1}H MRS glutamate levels associating positively with higher cognitive performance. The positive correlation between NAA and glutamate levels (**Figure 7B**) was consistent with prior reports in the normal brain [82], potentially underpinned by tight coupling of the two compounds in NAA synthesis in neuronal mitochondria by addition of glutamate-derived aspartate to an acetyl group derived from Acetyl-CoA, in a reaction catalyzed by L-aspartate-N-acetyltransferase [83]. Conversely, NAA has been postulated to serve as a reservoir of glutamate synthesis [84]. As an exploratory analysis, we observed a significant or trend group by visit interaction with increased GABA levels in left hippocampus with riluzole treatment. GABA is reportedly depleted in AD and mild cognitive impairment [85, 86]. Treatment-related increases in GABA levels **(Supplementary Figure 2B)** suggest that riluzole may at least partially alleviate this reported deficit, with possible benefit given the positive correlation of GABA with memory performance in this study (**Supplementary Figure 2C).** There was general agreement between the ratios of metabolite level peak ratios relative to unsuppressed water (W) and total creatine (tCr) in our study, but greater consistency in ratios measured relative to W. Caution has been urged in interpreting ratios relative to tCr because levels have been reported to change in a number of neuropsychiatric [87] and neurological disorders [88]. We provided both ratios for comparison with literature.

Riluzole was generally well tolerated, with no significant difference in side effects compared to placebo. Riluzole has been used for decades in the treatment of ALS. However, larger, longer duration studies are necessary to have a comprehensive evaluation of safety and efficacy of riluzole in the AD population, and should precede its use in AD outside of a monitored clinical trial.

This study has several limitations. First, the sample size was relatively small, and results require replication in larger-sample studies. A second limitation was the lack of amyloid characterization. However, the presence of an FDG PET AD pattern helped to confirm clinical diagnosis and has been shown to have a high degree of agreement with the presence of tau pathology [89]. Third, ^{1}H MRS is unable to differentiate neurotransmitter or vesicular

and metabolic pools of glutamate or GABA, limiting interpretation. ^{1}H MRS data acquisition techniques require relatively large voxels for reliable quantification of metabolites, potentially leading to partial volume effects and masking of group effects. As noted in other studies, longitudinal MRS measurements can be subject to technical variability and subject head motion. The study was not powered for neuropsychological outcome measurement, and clinical changes must be viewed only as directional and exploratory.

In conclusion, a slower decline in cerebral glucose metabolism was observed in riluzole-treated AD patients than in placebo in multiple AD-relevant brain regions, which correlated with cognitive performance. These findings support future fully powered clinical trials to further evaluate riluzole as a potential pharmacological therapy for AD.

Acknowledgements:

We thank patients and their families for their collaboration and help in this study. This trial was funded by Alzheimer's Drug Discovery Foundation and Dana Foundation (A.C.P.) with support from Mount Sinai Alzheimer's Disease Research Center P30AG066514 and P50AG05138-20, The Rockefeller University Grant # UL1 TR001866 from the National Center for Advancing Translational Sciences (NCATS), National Institutes of Health (NIH) Clinical and Translational Science Award (CTSA) program. A.C.P. is also funded by NIH R01 AG063819, NIH R01AG064020, Paul B. Beeson Emerging Leaders Career Development Award in Aging K76 AG054772, the BrightFocus Foundation, the DANA Foundation, the Alzheimer's Drug Discovery Foundation, the Alzheimer's Association, the Bernard L. Schwartz Award for Physician Scientist and the Karen Strauss Cook Research Scholar Award. D.C.S. received support from 1 R01 MH075895.
We thank Dr. Sam Gandy for recruitment support and Gargi Padki for research coordination support. We thank Muc Chieu Du, Simon Morim and Jojo Borja for their work in image data acquisition, and Laura Matthews for her assistance in preliminary analyses of the FDG PET data. We also thank Drs. Barbara O'Sullivan and Judith Neugroschl for blood test results revision.

Declaration of interests: A.C.P. has patent applications 41054762 and 63087610 related to riluzole. Rockefeller University through grant from the Alzheimer's Drug Discovery Foundation (ADDF) provided funds to ADM Diagnostics to D.C.M. for FDG PET analysis.

Icahn School of Medicine at Mount Sinai through ADDF grant provided funds to XsOsNMR consulting to D.C.S. for ^{1}H MRS analysis.

Author contributions: D.C.M., D.T., P.D.M., H.F., B.S.M., D.C.S. and A.C.P. designed the experiments. D.C.M. X.M., K.D., D.T., C.M., A.C.P. conducted experiments and acquired data; N.S., H.F., M.S., B.S.M. provided materials and data analysis tools; D.C.M., X.M., D.T., C.S.J., R.D.A., A.S.L., J.L., N.H., N.S., D.C.S. contributed to data analysis, D.C.M. and A.C.P. wrote the first version of the manuscript, D.C.M., D.T., C.S.J., D.C.S. and A.C.P. edited the manuscript.

References

1. 2020 Alzheimer's disease facts and figures. *Alzheimers Dement*. Mar 10 2020;doi:10.1002/alz.12068
2. Morrison JH, Hof PR. Life and death of neurons in the aging brain. Research Support, Non-U.S. Gov't
Research Support, U.S. Gov't, P.H.S.
Review. *Science*. Oct 17 1997;278(5337):412-9.
3. Morrison JH, Hof PR. Selective vulnerability of corticocortical and hippocampal circuits in aging and Alzheimer's disease. Review. *Progress in brain research*. 2002;136:467-86.
4. Crimins JL, Pooler A, Polydoro M, Luebke JI, Spires-Jones TL. The intersection of amyloid beta and tau in glutamatergic synaptic dysfunction and collapse in Alzheimer's disease. *Ageing Res Rev*. Jun 2013;12(3):757-63. doi:10.1016/j.arr.2013.03.002
5. Hof PR, Morrison JH. Quantitative analysis of a vulnerable subset of pyramidal neurons in Alzheimer's disease: II. Primary and secondary visual cortex. *J Comp Neurol*. Nov 1 1990;301(1):55-64. doi:10.1002/cne.903010106
6. Hof PR, Cox K, Morrison JH. Quantitative analysis of a vulnerable subset of pyramidal neurons in Alzheimer's disease: I. Superior frontal and inferior temporal cortex. *J Comp Neurol*. Nov 1 1990;301(1):44-54. doi:10.1002/cne.903010105
7. Morrison JH, Hof PR. Selective vulnerability of corticocortical and hippocampal circuits in aging and Alzheimer's disease. *Prog Brain Res*. 2002;136:467-86.
8. Hardingham GE, Bading H. Synaptic versus extrasynaptic NMDA receptor signalling: implications for neurodegenerative disorders. Research Support, Non-U.S. Gov't
Review. *Nature reviews Neuroscience*. Oct 2010;11(10):682-96. doi:10.1038/nrn2911
9. Hardingham GE, Fukunaga Y, Bading H. Extrasynaptic NMDARs oppose synaptic NMDARs by triggering CREB shut-off and cell death pathways. *Nat Neurosci*. May 2002;5(5):405-14. doi:10.1038/nn835

10. Sharma A, Kazim SF, Larson CS, et al. Divergent roles of astrocytic versus neuronal EAAT2 deficiency on cognition and overlap with aging and Alzheimer's molecular signatures. *Proc Natl Acad Sci U S A*. Oct 22 2019;116(43):21800-21811. doi:10.1073/pnas.1903566116
11. Braak H, Del Tredici K. Spreading of Tau Pathology in Sporadic Alzheimer's Disease Along Cortico-cortical Top-Down Connections. *Cereb Cortex*. Sep 1 2018;28(9):3372-3384. doi:10.1093/cercor/bhy152
12. Morrison JH, Hof PR. Life and death of neurons in the aging cerebral cortex. Research Support, N.I.H., Extramural
Review. *International review of neurobiology*. 2007;81:41-57. doi:10.1016/S0074-7742(06)81004-4
13. Hof PR, Morrison JH. Neocortical neuronal subpopulations labeled by a monoclonal antibody to calbindin exhibit differential vulnerability in Alzheimer's disease. *Exp Neurol*. Mar 1991;111(3):293-301. doi:10.1016/0014-4886(91)90096-u
14. Esclaire F, Lesort M, Blanchard C, Hugon J. Glutamate toxicity enhances tau gene expression in neuronal cultures. Research Support, Non-U.S. Gov't. *Journal of neuroscience research*. Aug 1 1997;49(3):309-18.
15. Sindou P, Lesort M, Couratier P, Yardin C, Esclaire F, Hugon J. Glutamate increases tau phosphorylation in primary neuronal cultures from fetal rat cerebral cortex. Research Support, Non-U.S. Gov't. *Brain research*. May 16 1994;646(1):124-8.
16. Pooler AM, Phillips EC, Lau DH, Noble W, Hanger DP. Physiological release of endogenous tau is stimulated by neuronal activity. Research Support, Non-U.S. Gov't. *EMBO reports*. Apr 2013;14(4):389-94. doi:10.1038/embor.2013.15
17. Yamada K, Holth JK, Liao F, et al. Neuronal activity regulates extracellular tau in vivo. *The Journal of experimental medicine*. Mar 10 2014;211(3):387-93. doi:10.1084/jem.20131685
18. Wu JW, Hussaini SA, Bastille IM, et al. Neuronal activity enhances tau propagation and tau pathology in vivo. *Nature neuroscience*. Aug 2016;19(8):1085-92. doi:10.1038/nn.4328
19. Li S, Hong S, Shepardson NE, Walsh DM, Shankar GM, Selkoe D. Soluble oligomers of amyloid Beta protein facilitate hippocampal long-term depression by disrupting neuronal glutamate uptake. In Vitro
Research Support, N.I.H., Extramural. *Neuron*. Jun 25 2009;62(6):788-801. doi:10.1016/j.neuron.2009.05.012
20. Li S, Jin M, Koeglsperger T, Shepardson NE, Shankar GM, Selkoe DJ. Soluble Abeta oligomers inhibit long-term potentiation through a mechanism involving excessive activation of extrasynaptic NR2B-containing NMDA receptors. Research Support, N.I.H., Extramural. *The Journal of neuroscience : the official journal of the Society for Neuroscience*. May 4 2011;31(18):6627-38. doi:10.1523/JNEUROSCI.0203-11.2011
21. Kamenetz F, Tomita T, Hsieh H, et al. APP processing and synaptic function. *Neuron*. Mar 27 2003;37(6):925-37.
22. Snyder EM, Nong Y, Almeida CG, et al. Regulation of NMDA receptor trafficking by amyloid-beta. Research Support, N.I.H., Extramural

Research Support, Non-U.S. Gov't
Research Support, U.S. Gov't, P.H.S. *Nature neuroscience*. Aug 2005;8(8):1051-8. doi:10.1038/nn1503
23. Pereira AC, Lambert HK, Grossman YS, et al. Glutamatergic regulation prevents hippocampal-dependent age-related cognitive decline through dendritic spine clustering. *Proceedings of the National Academy of Sciences of the United States of America*. Dec 30 2014;111(52):18733-8. doi:10.1073/pnas.1421285111
24. Govindarajan A, Kelleher RJ, Tonegawa S. A clustered plasticity model of long-term memory engrams. *Nat Rev Neurosci*. Jul 2006;7(7):575-83. doi:10.1038/nrn1937
25. Larkum ME, Nevian T. Synaptic clustering by dendritic signalling mechanisms. *Curr Opin Neurobiol*. Jun 2008;18(3):321-31. doi:10.1016/j.conb.2008.08.013
26. Pereira AC, Gray JD, Kogan JF, et al. Age and Alzheimer's disease gene expression profiles reversed by the glutamate modulator riluzole. *Molecular psychiatry*. Mar 29 2016;doi:10.1038/mp.2016.33
27. Okamoto M, Gray JD, Larson CS, et al. Riluzole reduces amyloid beta pathology, improves memory, and restores gene expression changes in a transgenic mouse model of early-onset Alzheimer's disease. *Transl Psychiatry*. Aug 14 2018;8(1):153. doi:10.1038/s41398-018-0201-z
28. Colonna M, Wang Y. TREM2 variants: new keys to decipher Alzheimer disease pathogenesis. *Nat Rev Neurosci*. Apr 2016;17(4):201-7. doi:10.1038/nrn.2016.7
29. Streit WJ. Microglia and Alzheimer's disease pathogenesis. *J Neurosci Res*. Jul 1 2004;77(1):1-8. doi:10.1002/jnr.20093
30. Butovsky O, Jedrychowski MP, Moore CS, et al. Identification of a unique TGF-beta-dependent molecular and functional signature in microglia. *Nat Neurosci*. Jan 2014;17(1):131-43. doi:10.1038/nn.3599
31. Keren-Shaul H, Spinrad A, Weiner A, et al. A Unique Microglia Type Associated with Restricting Development of Alzheimer's Disease. *Cell*. Jun 15 2017;169(7):1276-1290 e17. doi:10.1016/j.cell.2017.05.018
32. Hunsberger HC, Weitzner DS, Rudy CC, et al. Riluzole rescues glutamate alterations, cognitive deficits, and tau pathology associated with P301L tau expression. *Journal of neurochemistry*. Jul 4 2015;doi:10.1111/jnc.13230
33. Pontecorvo MJ, Devous MD, Kennedy I, et al. A multicentre longitudinal study of flortaucipir (18F) in normal ageing, mild cognitive impairment and Alzheimer's disease dementia. *Brain*. Jun 1 2019;142(6):1723-1735. doi:10.1093/brain/awz090
34. Cao YJ, Dreixler JC, Couey JJ, Houamed KM. Modulation of recombinant and native neuronal SK channels by the neuroprotective drug riluzole. *Eur J Pharmacol*. Aug 2 2002;449(1-2):47-54. doi:10.1016/s0014-2999(02)01987-8
35. Urbani A, Belluzzi O. Riluzole inhibits the persistent sodium current in mammalian CNS neurons. *Eur J Neurosci*. Oct 2000;12(10):3567-74. doi:10.1046/j.1460-9568.2000.00242.x
36. Katoh-Semba R, Asano T, Ueda H, et al. Riluzole enhances expression of brain-derived neurotrophic factor with consequent proliferation of granule

precursor cells in the rat hippocampus. *FASEB J*. Aug 2002;16(10):1328-30. doi:10.1096/fj.02-0143fje
37. Mizuta I, Ohta M, Ohta K, Nishimura M, Mizuta E, Kuno S. Riluzole stimulates nerve growth factor, brain-derived neurotrophic factor and glial cell line-derived neurotrophic factor synthesis in cultured mouse astrocytes. *Neurosci Lett*. Sep 14 2001;310(2-3):117-20. doi:10.1016/s0304-3940(01)02098-5
38. Chowdhury GM, Banasr M, de Graaf RA, Rothman DL, Behar KL, Sanacora G. Chronic riluzole treatment increases glucose metabolism in rat prefrontal cortex and hippocampus. Research Support, N.I.H., Extramural. *Journal of cerebral blood flow and metabolism : official journal of the International Society of Cerebral Blood Flow and Metabolism*. Dec 2008;28(12):1892-7. doi:10.1038/jcbfm.2008.78
39. Banasr M, Chowdhury GM, Terwilliger R, et al. Glial pathology in an animal model of depression: reversal of stress-induced cellular, metabolic and behavioral deficits by the glutamate-modulating drug riluzole. *Molecular psychiatry*. May 2010;15(5):501-11. doi:10.1038/mp.2008.106
40. Fumagalli E, Funicello M, Rauen T, Gobbi M, Mennini T. Riluzole enhances the activity of glutamate transporters GLAST, GLT1 and EAAC1. *European journal of pharmacology*. Jan 14 2008;578(2-3):171-6. doi:10.1016/j.ejphar.2007.10.023
41. Frizzo ME, Dall'Onder LP, Dalcin KB, Souza DO. Riluzole enhances glutamate uptake in rat astrocyte cultures. *Cell Mol Neurobiol*. Feb 2004;24(1):123-8.
42. Sibson NR, Dhankhar A, Mason GF, Rothman DL, Behar KL, Shulman RG. Stoichiometric coupling of brain glucose metabolism and glutamatergic neuronal activity. *Proc Natl Acad Sci U S A*. Jan 6 1998;95(1):316-21. doi:10.1073/pnas.95.1.316
43. Shen J, Petersen KF, Behar KL, et al. Determination of the rate of the glutamate/glutamine cycle in the human brain by in vivo 13C NMR. *Proc Natl Acad Sci U S A*. Jul 6 1999;96(14):8235-40. doi:10.1073/pnas.96.14.8235
44. Magistretti PJ. Role of glutamate in neuron-glia metabolic coupling. *Am J Clin Nutr*. Sep 2009;90(3):875S-880S. doi:10.3945/ajcn.2009.27462CC
45. Patel AB, Lai JC, Chowdhury GM, et al. Direct evidence for activity-dependent glucose phosphorylation in neurons with implications for the astrocyte-to-neuron lactate shuttle. *Proc Natl Acad Sci U S A*. Apr 8 2014;111(14):5385-90. doi:10.1073/pnas.1403576111
46. McKhann G, Drachman D, Folstein M, Katzman R, Price D, Stadlan EM. Clinical diagnosis of Alzheimer's disease: report of the NINCDS-ADRDA Work Group under the auspices of Department of Health and Human Services Task Force on Alzheimer's Disease. Guideline
Practice Guideline. *Neurology*. Jul 1984;34(7):939-44.
47. McKhann GM, Knopman DS, Chertkow H, et al. The diagnosis of dementia due to Alzheimer's disease: recommendations from the National Institute on Aging-Alzheimer's Association workgroups on diagnostic guidelines for Alzheimer's disease. Consensus Development Conference, NIH
Research Support, Non-U.S. Gov't. *Alzheimer's & dementia : the journal of the Alzheimer's Association*. May 2011;7(3):263-9. doi:10.1016/j.jalz.2011.03.005
48. Rosen WG, Mohs RC, Davis KL. A new rating scale for Alzheimer's disease. Research Support, U.S. Gov't, Non-P.H.S.

Research Support, U.S. Gov't, P.H.S. *The American journal of psychiatry*. Nov 1984;141(11):1356-64.
49. Mohs RC, Knopman D, Petersen RC, et al. Development of cognitive instruments for use in clinical trials of antidementia drugs: additions to the Alzheimer's Disease Assessment Scale that broaden its scope. The Alzheimer's Disease Cooperative Study. Research Support, U.S. Gov't, P.H.S. *Alzheimer disease and associated disorders*. 1997;11 Suppl 2:S13-21.
50. Galasko D, Bennett D, Sano M, et al. An inventory to assess activities of daily living for clinical trials in Alzheimer's disease. The Alzheimer's Disease Cooperative Study. Clinical Trial
Research Support, U.S. Gov't, P.H.S. *Alzheimer disease and associated disorders*. 1997;11 Suppl 2:S33-9.
51. Cummings JL, Mega M, Gray K, Rosenberg-Thompson S, Carusi DA, Gornbein J. The Neuropsychiatric Inventory: comprehensive assessment of psychopathology in dementia. Research Support, Non-U.S. Gov't
Research Support, U.S. Gov't, Non-P.H.S.
Research Support, U.S. Gov't, P.H.S. *Neurology*. Dec 1994;44(12):2308-14.
52. Matthews DC, Lukic AS, Andrews RD, et al. Dissociation of Down syndrome and Alzheimer's disease effects with imaging. *Alzheimers Dement (N Y)*. Jun 2016;2(2):69-81. doi:10.1016/j.trci.2016.02.004
53. Peters F, Perani D, Herholz K, et al. Orbitofrontal dysfunction related to both apathy and disinhibition in frontotemporal dementia. *Dement Geriatr Cogn Disord*. 2006;21(5-6):373-9. doi:10.1159/000091898
54. Mega MS, Dinov ID, Porter V, et al. Metabolic patterns associated with the clinical response to galantamine therapy: a fludeoxyglucose f 18 positron emission tomographic study. *Arch Neurol*. May 2005;62(5):721-8. doi:10.1001/archneur.62.5.721
55. Maass A, Landau S, Baker SL, et al. Comparison of multiple tau-PET measures as biomarkers in aging and Alzheimer's disease. *Neuroimage*. Aug 15 2017;157:448-463. doi:10.1016/j.neuroimage.2017.05.058
56. Fischl B, Salat DH, Busa E, et al. Whole brain segmentation: automated labeling of neuroanatomical structures in the human brain. *Neuron*. Jan 31 2002;33(3):341-55. doi:10.1016/s0896-6273(02)00569-x
57. Tzourio-Mazoyer N, Landeau B, Papathanassiou D, et al. Automated anatomical labeling of activations in SPM using a macroscopic anatomical parcellation of the MNI MRI single-subject brain. *Neuroimage*. Jan 2002;15(1):273-89. doi:10.1006/nimg.2001.0978
58. Romano S, Coarelli G, Marcotulli C, et al. Riluzole in patients with hereditary cerebellar ataxia: a randomised, double-blind, placebo-controlled trial. *Lancet Neurol*. Oct 2015;14(10):985-91. doi:10.1016/S1474-4422(15)00201-X
59. Dreher W, Leibfritz D. Detection of homonuclear decoupled in vivo proton NMR spectra using constant time chemical shift encoding: CT-PRESS. *Magnetic resonance imaging*. Jan 1999;17(1):141-50.
60. Mayer D, Spielman DM. Detection of glutamate in the human brain at 3 T using optimized constant time point resolved spectroscopy. *Magnetic resonance in*

medicine : official journal of the Society of Magnetic Resonance in Medicine / Society of Magnetic Resonance in Medicine. Aug 2005;54(2):439-42. doi:10.1002/mrm.20571
61. Girgis RR, Baker S, Mao X, et al. Effects of acute N-acetylcysteine challenge on cortical glutathione and glutamate in schizophrenia: A pilot in vivo proton magnetic resonance spectroscopy study. *Psychiatry Res*. May 2019;275:78-85. doi:10.1016/j.psychres.2019.03.018
62. Shungu DC, Mao X, Gonzales R, et al. Brain gamma-aminobutyric acid (GABA) detection in vivo with the J-editing (1) H MRS technique: a comprehensive methodological evaluation of sensitivity enhancement, macromolecule contamination and test-retest reliability. *NMR in biomedicine*. Jul 2016;29(7):932-42. doi:10.1002/nbm.3539
63. Landau SM, Harvey D, Madison CM, et al. Associations between cognitive, functional, and FDG-PET measures of decline in AD and MCI. *Neurobiol Aging*. Jul 2011;32(7):1207-18. doi:10.1016/j.neurobiolaging.2009.07.002
64. Khosravi M, Peter J, Wintering NA, et al. 18F-FDG Is a Superior Indicator of Cognitive Performance Compared to 18F-Florbetapir in Alzheimer's Disease and Mild Cognitive Impairment Evaluation: A Global Quantitative Analysis. *J Alzheimers Dis*. 2019;70(4):1197-1207. doi:10.3233/JAD-190220
65. Alexander GE, Chen K, Pietrini P, Rapoport SI, Reiman EM. Longitudinal PET Evaluation of Cerebral Metabolic Decline in Dementia: A Potential Outcome Measure in Alzheimer's Disease Treatment Studies. Comparative Study
Research Support, Non-U.S. Gov't
Research Support, U.S. Gov't, P.H.S. *The American journal of psychiatry*. May 2002;159(5):738-45.
66. Pereira AC, Lambert HK, Grossman YS, et al. Glutamatergic regulation prevents hippocampal-dependent age-related cognitive decline through dendritic spine clustering. *Proceedings of the National Academy of Sciences of the United States of America*. Dec 30 2014;111(52):18733-8. doi:10.1073/pnas.1421285111
67. Wang T, Huang Q, Reiman EM, et al. Effects of memantine on clinical ratings, fluorodeoxyglucose positron emission tomography measurements, and cerebrospinal fluid assays in patients with moderate to severe Alzheimer dementia: a 24-week, randomized, clinical trial. *J Clin Psychopharmacol*. Oct 2013;33(5):636-42. doi:10.1097/JCP.0b013e31829a876a
68. Revett TJ, Baker GB, Jhamandas J, Kar S. Glutamate system, amyloid ss peptides and tau protein: functional interrelationships and relevance to Alzheimer disease pathology. *J Psychiatry Neurosci*. Jan 2013;38(1):6-23. doi:10.1503/jpn.110190
69. Lipton SA. The molecular basis of memantine action in Alzheimer's disease and other neurologic disorders: low-affinity, uncompetitive antagonism. *Curr Alzheimer Res*. Apr 2005;2(2):155-65. doi:10.2174/1567205053585846
70. Mosconi L, Tsui WH, Herholz K, et al. Multicenter standardized 18F-FDG PET diagnosis of mild cognitive impairment, Alzheimer's disease, and other dementias. *J Nucl Med*. Mar 2008;49(3):390-8. doi:10.2967/jnumed.107.045385
71. Minoshima S, Giordani B, Berent S, Frey KA, Foster NL, Kuhl DE. Metabolic reduction in the posterior cingulate cortex in very early Alzheimer's disease. *Ann Neurol*. Jul 1997;42(1):85-94. doi:10.1002/ana.410420114

72. Mutlu J, Landeau B, Tomadesso C, et al. Connectivity Disruption, Atrophy, and Hypometabolism within Posterior Cingulate Networks in Alzheimer's Disease. *Front Neurosci*. 2016;10:582. doi:10.3389/fnins.2016.00582
73. Koelewijn L, Lancaster TM, Linden D, et al. Oscillatory hyperactivity and hyperconnectivity in young APOE-varepsilon4 carriers and hypoconnectivity in Alzheimer's disease. *Elife*. Apr 30 2019;8doi:10.7554/eLife.36011
74. Nuriel T, Angulo SL, Khan U, et al. Neuronal hyperactivity due to loss of inhibitory tone in APOE4 mice lacking Alzheimer's disease-like pathology. *Nat Commun*. Nov 13 2017;8(1):1464. doi:10.1038/s41467-017-01444-0
75. Graff-Radford J, Kantarci K. Magnetic resonance spectroscopy in Alzheimer's disease. *Neuropsychiatric disease and treatment*. 2013;9:687-96. doi:10.2147/NDT.S35440
76. Schmidt R, Ropele S, Pendl B, et al. Longitudinal multimodal imaging in mild to moderate Alzheimer disease: a pilot study with memantine. *J Neurol Neurosurg Psychiatry*. Dec 2008;79(12):1312-7. doi:10.1136/jnnp.2007.141648
77. Penner J, Rupsingh R, Smith M, Wells JL, Borrie MJ, Bartha R. Increased glutamate in the hippocampus after galantamine treatment for Alzheimer disease. *Prog Neuropsychopharmacol Biol Psychiatry*. Feb 1 2010;34(1):104-10. doi:10.1016/j.pnpbp.2009.10.007
78. Kalra S. Magnetic Resonance Spectroscopy in ALS. *Front Neurol*. 2019;10:482. doi:10.3389/fneur.2019.00482
79. Schott JM, Frost C, MacManus DG, Ibrahim F, Waldman AD, Fox NC. Short echo time proton magnetic resonance spectroscopy in Alzheimer's disease: a longitudinal multiple time point study. *Brain*. Nov 2010;133(11):3315-22. doi:10.1093/brain/awq208
80. Fayed N, Modrego PJ, Rojas-Salinas G, Aguilar K. Brain glutamate levels are decreased in Alzheimer's disease: a magnetic resonance spectroscopy study. Research Support, Non-U.S. Gov't. *American journal of Alzheimer's disease and other dementias*. Sep 2011;26(6):450-6. doi:10.1177/1533317511421780
81. Hattori N, Abe K, Sakoda S, Sawada T. Proton MR spectroscopic study at 3 Tesla on glutamate/glutamine in Alzheimer's disease. *Neuroreport*. Jan 21 2002;13(1):183-6.
82. Kraguljac NV, Reid MA, White DM, den Hollander J, Lahti AC. Regional decoupling of N-acetyl-aspartate and glutamate in schizophrenia. *Neuropsychopharmacology*. Nov 2012;37(12):2635-42. doi:10.1038/npp.2012.126
83. Birken DL, Oldendorf WH. N-acetyl-L-aspartic acid: a literature review of a compound prominent in 1H-NMR spectroscopic studies of brain. *Neurosci Biobehav Rev*. Spring 1989;13(1):23-31. doi:10.1016/s0149-7634(89)80048-x
84. Clark JF, Doepke A, Filosa JA, et al. N-acetylaspartate as a reservoir for glutamate. *Med Hypotheses*. 2006;67(3):506-12. doi:10.1016/j.mehy.2006.02.047
85. Gueli MC, Taibi G. Alzheimer's disease: amino acid levels and brain metabolic status. *Neurol Sci*. Sep 2013;34(9):1575-9. doi:10.1007/s10072-013-1289-9
86. Bai X, Edden RA, Gao F, et al. Decreased gamma-aminobutyric acid levels in the parietal region of patients with Alzheimer's disease. *J Magn Reson Imaging*. May 2015;41(5):1326-31. doi:10.1002/jmri.24665

87. Ongur D, Prescot AP, Jensen JE, Cohen BM, Renshaw PF. Creatine abnormalities in schizophrenia and bipolar disorder. *Psychiatry Res*. Apr 30 2009;172(1):44-8. doi:10.1016/j.pscychresns.2008.06.002
88. Weiduschat N, Mao X, Hupf J, et al. Motor cortex glutathione deficit in ALS measured in vivo with the J-editing technique. *Neurosci Lett*. Jun 6 2014;570:102-7. doi:10.1016/j.neulet.2014.04.020
89. Matthews DC, Ritter A, Thomas RG, et al. Rasagiline effects on glucose metabolism, cognition, and tau in Alzheimer's dementia. *Alzheimers Dement (N Y)*. 2021;7(1):e12106. doi:10.1002/trc2.12106

Figure legends:

Figure 1. **A. [i]** Pre-specified regions of interest, which were masked with each subject's gray tissue segment, in addition to a region defined to include the same tissue as the MRI PC region, **[ii]** AD progression classifier pattern, in which increasing progression scores reflect increasing expression of the pattern (subset shown) of hypometabolism (blue) and preservation (red) relative to whole brain. The progression scores of 517 test subjects from amyloid negative cognitively normal status through amyloid positive Early MCI (EMCI), late MCI (LMCI) and Alzheimer's dementia (AD) are shown, with mean and standard error, illustrating the correspondence between increased score and worsening clinical severity (data derived using FDG PET scans from ADNI, www.adni-info.org, as described in Matthews et al, 2016).

B. **[i]** Axial, **[ii]** sagittal and **[iii]** coronal MR images of a human brain, with depiction of the size and placement of the voxel of interest in the posterior cingulate cortex (PC). PC voxel dimensions: 2.0 cm (anterior-posterior) x 2.0 cm (left-right) x 2.0 cm (superior-inferior), or $8cm^3$. **[iv]** Sample CT-PRESS MRS data from the PC voxel, showing (a) an experimental spectrum with a clearly resolved C-4 glutamate (Glu) resonance at 2.35 ppm, as well as the resonances for N-acetyl-L-aspartate (NAA), total creatine (tCr), total choline (tCho) and combined resonances of C-2 glutamate and C-2 glutamine (Glx); (b) model fitting of spectrum in (a) to obtain the metabolite peak areas of interest; (c) individual components of the model-fitted spectrum in (a); (d) residuals of the difference between spectra in (a) and in (b).

Figure 2: Enrollment, radomization and trial completion

Figure 3. (A) Posterior cingulate (PC) region of interest (representative sagittal slice) in FDG PET; (B) Comparison between placebo and riluzole treated arms of the absolute and percentage change in PC FDG SUVR over the 6-month treatment period; (C) Individual change from baseline to follow up in PC SUVR in placebo (left) and riluzole (right) treated arms; (D) Comparison of change in PC SUVR by ApoE4 carrier and non-carrier subgroups,

and by younger and older age groups. Individual values are shown with mean and standard error bars.

Figure 4. (A) Region of interest boundaries shown in representative slices, color-coded to indicate the significance levels in comparisons between placebo and riluzole treated arms of the 6 month change in FDG SUVR; (B) Comparison between placebo and riluzole treated arms of the 6 month change in FDG SUVR for posterior cingulate (PostCing), combined PC and precuneus (PCC), lateral temporal (LatTemp), right hippocampus (Hip), orbitofrontal (OrbFrontal), Frontal, Parietal, and subcortical white matter (as a comparator, expected to remain stable). Individual values are shown with mean and standard error bars.

Figure 5. (A) Comparison between placebo and riluzole treated arms of the change in FDG Progression score. (B) Correlation between AD Progression score at baseline and ADAScog score at baseline (left) and between 6 month change in AD progression score and in ADAS cog (right) for all study participants.

Figure 6. Correlations at baseline between: (A) FDG AD Progression score and MMSE score; (B) posterior cingulate-precuneus (PCC) score and MMSE score; (C) lateral temporal FDG SUVR and ADAScog score; (D) orbitofrontal FDG SUVR and Neuropsychiatric Inventory (NPI) score.

Figure 7: A: ^{1}H MRS measures of Glu/W (top) and Glu/tCr (bottom) levels changes in posterior cingulate at baseline, 3 months and 6 months (B) Correlations at baseline, midpoint and endpoint between NAA/W and Glu/W in riluzole and placebo groups (top) and NAA/tCr and Glu/tCr in riluzole and placebo groups (bottom). (C) Correlations at baseline between Glu/W and MMSE (top) and Glu/W and ADAScog (bottom) across subjects.

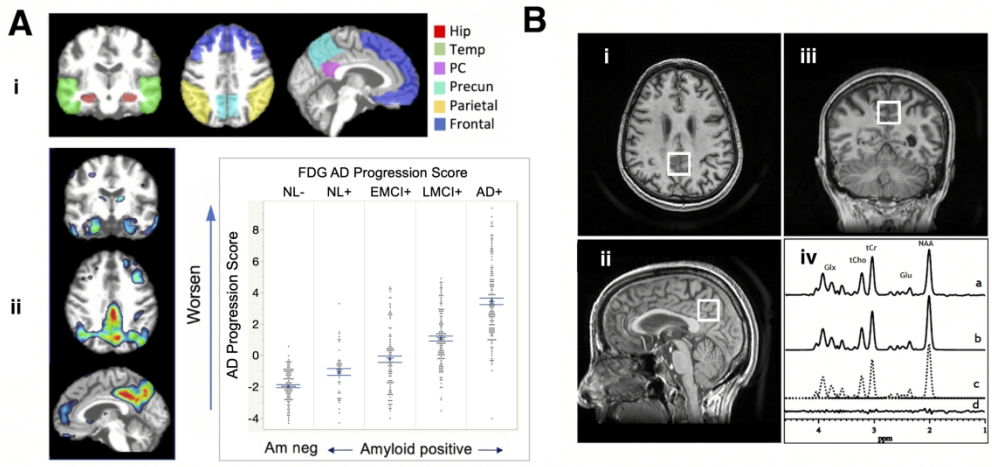

Figure 1

273x138mm (300 x 300 DPI)

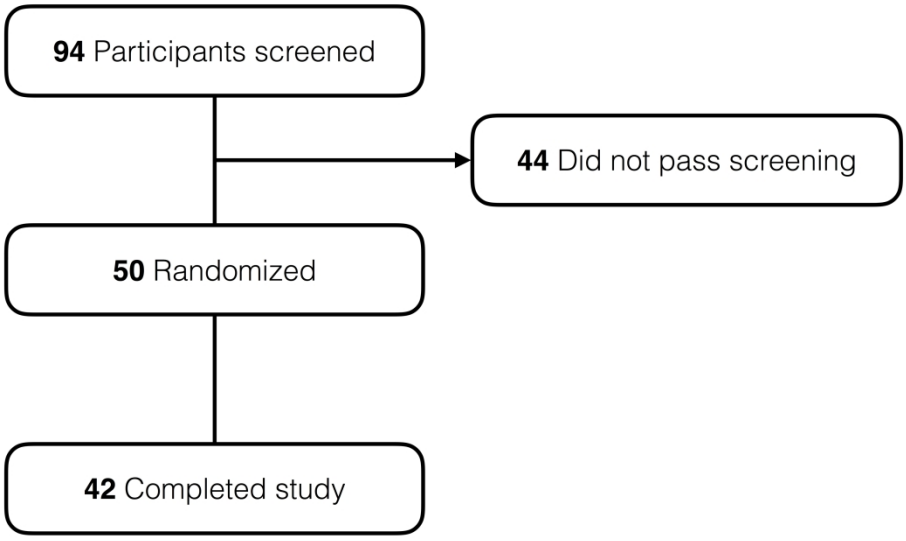

Figure 2

346x208mm (300 x 300 DPI)

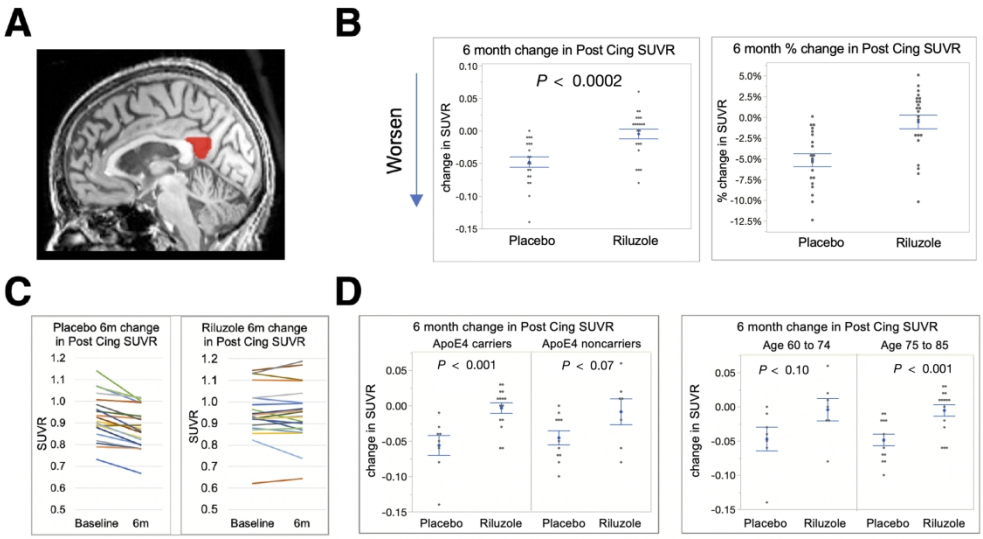

Figure 3

276x164mm (300 x 300 DPI)

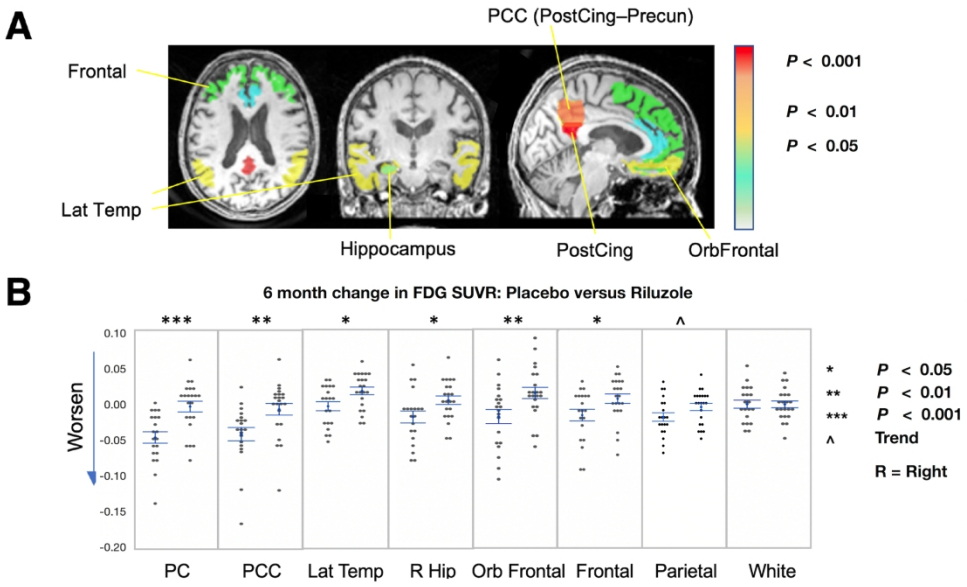

Figure 4

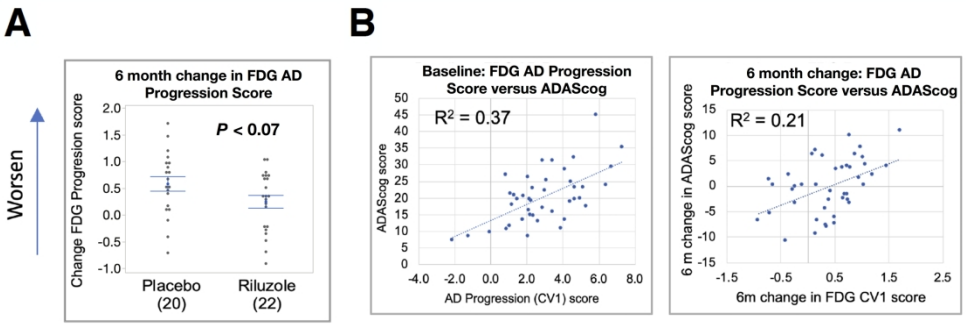

Figure 5

271x98mm (300 x 300 DPI)

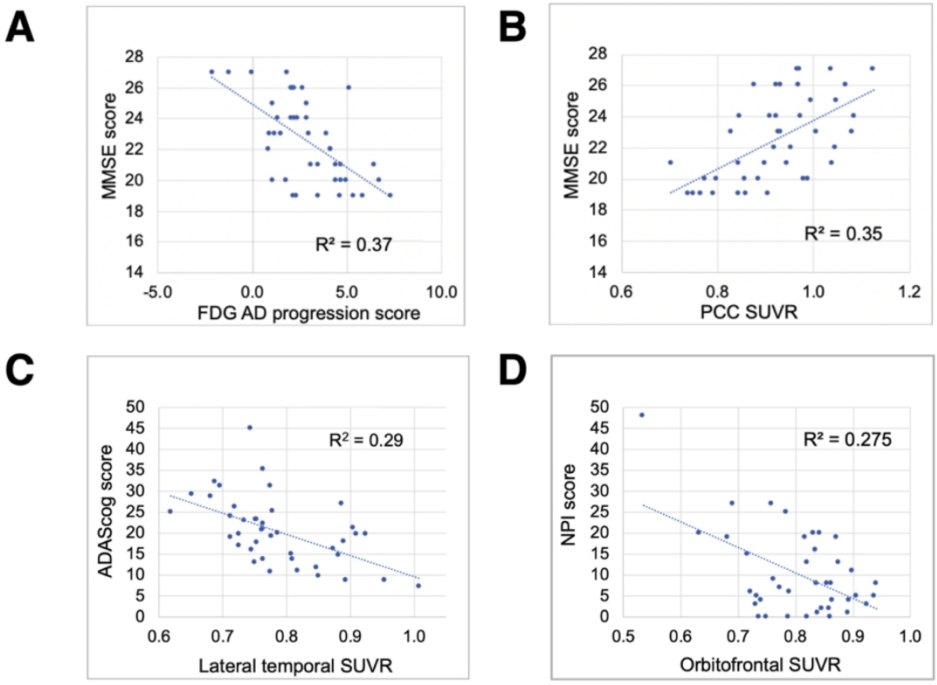

Figure 6

304x215mm (300 x 300 DPI)

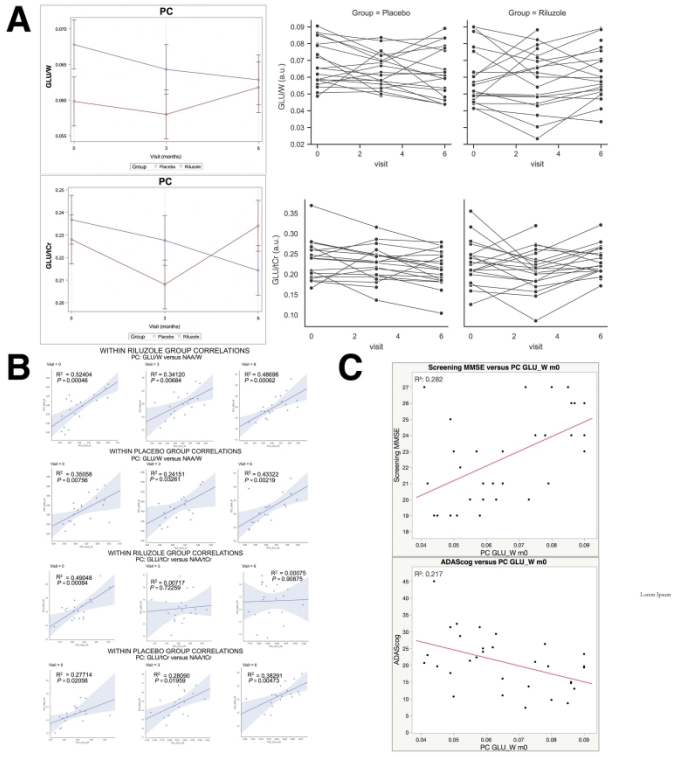

Figure 7

361x270mm (300 x 300 DPI)

Table 1 Demographic and baseline clinical characteristics

Characteristic	Placebo (n = 20)	Riluzole (n = 22)	P-value
Age, years, mean ± SD	74.6 ± 7.7	75.3 ± 5.8	0.73
Sex, n (%)			0.30
Female	14 (70.0)	12 (54.5)	
Male	6 (30.0)	10 (45.5)	
Race/ethnicity, n (%)			1.00
Black or African American	0 (0)	1 (4.5)	
Black/non-Hispanic	1 (5.0)	0 (0)	
Latino/Hispanic	0 (0)	1 (4.5)	
White/non-Hispanic	19 (95.0)	20 (90.9)	
Education, years, mean ± SD	15.1 ± 3.1	15.9 ± 3.0	0.39
ApoE4 carrier, n (%)	8 (40.0)	15 (68.2)	0.11
Clinical scales, mean ± SD			
ADAS-cog	17.9 ± 7.5	22.5 ± 7.9	0.08
ADL total	68.1 ± 9.3	68.4 ± 9.5	0.91
CDR-sum of boxes	3.6 ± 1.8	3.8 ± 1.9	0.73
CDR total	0.6 ± 0.2	0.6 ± 0.2	0.59
MMSE	22.8 ± 2.9	22.5 ± 2.5	0.72
NPI	10.2 ± 11.1	9.6 ± 9.2	0.86
GDS	5.3 ± 3.7	5.2 ± 6.6	0.98

ADAS-cog = Alzheimer's Disease Assessment Scale; ADL = Activities of Daily Living Inventory scale; CDR = Clinical Dementia Rating scale; GDS = Geriatric Depression Scale; MMSE = Mini–Mental State Examination; NPI = Neuropsychiatric Inventory score.